BARYON ACOUSTIC OSCILLATION AND LSS FORMATION IN THE NASCENT UNIVERSE

THESIS SUBMITTED TO

The Department of Mathematics and Natural Sciences, BRAC University in partial fulfilment for the requirements of the award of the degree of

Bachelor of Science in Physics

By

AOM Mushfeque Un Nabi

Department of Mathematics and Natural Sciences

BRAC University

2017

DECLARATION

I do hereby declare that the thesis titled "BARYON ACOUSTIC OSCILLATION AND LSS FORMATION IN THE NASCENT UNIVERSE" is submitted to the Department of Mathematics and Natural Sciences of BRAC University, in partial fulfilment for the requirements of the Bachelor of Science degree in Physics. This thesis paper is the work of my own and has not been submitted elsewhere for any other degree or diploma award. All sources used as reference have been cited and acknowledged within the text appropriately.

_____

Candidate
AOM Mushfeque Un Nabi
ID: 06311002

_____

Certified
Professor Arshad Momen
Department of Theoretical Physics
University of Dhaka

Acknowledgements

I would like to thank my parents, teachers and friends for guiding me along this very difficult journey which we refer to as “life”.

The person I would like mention foremost in remembrance is the Late Professor Mofiz-uddin Ahmed, who guided me in writing the introduction. My course teachers Dr. Dipen Bhattacharya and Professor A.A.Ziauddin Ahmed suggested the topic of the thesis. I am most grateful to Professor Arshad Momen for certifying this paper and helping me at many situations in my personal and professional life. I would be stranded without him.

I would also like to acknowledge Dr. Amin Hasan Kazi, Dr. Aparna Islam, Professor Firdous Azim, Professor Kaiser Haq, Ms. Sharmina Hussain, Mr. Iftekhar Md. Shafiqul Kalam, Md. Maruf Ahmed, Ms. Moushumi Zahur, Mr. Mahabobe Sobhani, Muhammad Lutfor Rahman, Khandaker Mahmudul Hasan (Liton Sir) and Mushira Habib for being my subject teachers over the years at the University.

I am thankful to my friends Sunitra Hawlader, Galib Ahsan, Shudipto Amin, Khalid Hossain and Nakib Haider for looking out for me.

And last but not the least, I express my sincerest gratitude and respects to my school teachers who brought me up throughout the years; Mrs. Niloufer Manzur, Mrs. Shamina Mainuddin, Ms. Leena Kabir, Mrs. Suraiya Ehsan, Mr. Abdul Quader, Mrs. Najma Alam, Ms. Tahsina Shamsunnahar, Ms. Rebeka Majid, Ms. Tasneem Athar, Professor Md. Kutubuddin, Professor Bibhangshu Biswas, Professor Swapan Kumar Mondal and Mr. Syed Ahmed Zahir.

The list of names is quite long and I have tried to fit in as many as I can here. Those that I have missed please understand that the human brain comes with its limitations.

Thank you!

Abstract

The Cosmic Microwave Background Radiation (CMBR) and cosmological redshift are together regarded as the best available evidence for the Big Bang theory. Measurements of this radiation have made the inflationary Big Bang theory the standard model of the primitive universe. These measurements are conducted by cosmic detectors sent by astronomers into space (via satellites). The CMB consists of anisotropies (irregularities) which are present across the sky. The anisotropy of the CMB consists of the small temperature fluctuations in the blackbody left over from the Big Bang (average temperature 2.725K as measured by FIRAS on COBE). The fluctuations lie over a region known as the surface of last scattering, where the CMB photons were scattered for the last time before being detected. The anisotropy of the cosmic microwave background is divided as:

1. Primary anisotropy, (due to effects which occur at the last scattering surface and before)
2. Secondary anisotropy (due to effects such as interactions of the background radiation with hot gas or gravitational potentials, which occur between the last scattering surface and the observer)

The structure of the cosmic microwave anisotropies is principally determined by two effects: **acoustic oscillations** and **diffusion damping**. In the first part of the thesis a description of the primary anisotropy of the CMBR will be detailed. Data analysis and mathematical derivations will be cited in the second part where the relevant power spectra and diffusion damping oscillation graphs will be shown. Finally, the results based on seven years of data from the Wilkinson Microwave Anisotropy Probe (WMAP) shall be presented and any theories regarding future research will be stated.

Contents

5. Figures

1. Introduction

`The evolution of the world can be compared to a display of fireworks

that has just ended; some few red wisps, ashes and smoke.

Standing on a cooled cinder, we see the slow fading of the suns,

and we try to recall the vanishing brilliance

of the origin of the worlds.' ——*Lemaitre*

The expansion of the universe is the most imposing discovery of modern science. Today it is a firmly established concept and the only debate centres on the way this is taking place. It was first suggested by the general theory of relativity and is backed up by physics in the examination of the galactic (power) towards the red section spectrum; the regular movement of their spectrum may be explained by the distancing of one galaxy from another.

Thus the size of the universe is probably constantly increasing and this increase becomes bigger for galaxies which are further away from us.

The speeds at which these celestial bodies are moving may, in the course of this perpetual expansion, go from fractions of the speed of light to speeds faster than this.[1]

1.1 Cosmic sound

The universe looks the same around each point and in each direction and in the beginning, there were neutrinos, lots of neutrinos. The temperature was 3000K (z = 1100) There still are neutrinos, only we couldn't detect them until a few decades ago. We had some idea of their presence, for without them we could not account for the remainder of the mass of the universe, as only (today) roughly 5% of the entire universe consists of visible light matter. With these neutrinos were antineutrinos, photons and the first nucleons and electrons.

Under the intense conditions of the early universe, ionized matter gave off radiation that was trapped within it like light in a dense fog. Then, when the universe was about 400,000 years old, dark matter ruled all known space and for every atom in the universe there were 2 photons, 1 neutrino and 6 dark matter particles.

As the universe expanded and cooled, electrons and protons came together to form neutral atoms, and matter lost its ability to ensnare light. The universe lost its opacity. Today, some 14 billion years later, the photons from that great release of radiation have reached us in the form of cosmic microwave background radiation (CMBR). The sky is at 2.73K, and the effects of the mysterious dark matter appear to be the result of an invisible mass of the remainder of the universe. Where did so much matter come from? That is what we as cosmologists are trying to find out!

The process in which protons and electrons recombine at $z_* = 1100$ (Figure 4.2) leaving a low level of outstanding ions is typical for how the cooling universe leaves relic particles. At very high temperatures, each reaction is in approximate equilibrium with the opposite reaction and the particles are in equilibrium. As the temperature changes, the equilibrium values change, but as the reaction rate is high, the particles quickly adapt to the new equilibrium.

If we tune a television set between channels, about 1 percent of the static we see on the screen is from the CMB. When astronomers scan the sky for these microwaves, they find that the signal looks almost identical in every direction. The ubiquity and constancy of the CMB is a sign that it comes from a simpler past, long before structures such as planets, stars and galaxies formed. Because of this simplicity, we can predict the properties of the CMB to exquisite accuracy. And in the past few years, cosmologists have been able to compare these predictions with increasingly precise observations from microwave telescopes carried by balloons and spacecraft. This research has brought us closer to answering some age-old questions such as 'When did the galaxies form? What is the universe made of? How old is it?'

Arno Penzias and Robert Wilson of AT&T Bell Laboratories detected the CMB radiation in 1965 while trying to find the source of a mysterious background noise in their radio antenna. The discovery firmly established the big bang theory, which states that the early universe was a hot, dense plasma of charged particles and photons. Since that time, the CMBR has been cooled by the expansion of the universe, and it is extremely cold today and comparable to the radiation released by a body at a temperature of 2.7K. But when the CMBR was released, its temperature was nearly 3,000K (or about 2,727°C).

In 1990, a satellite called COBE (for Cosmic Background Explorer) measured the spectrum of the CMB radiation, showing it to have exactly the expected form i.e. of a blackbody. Overshadowing this impressive achievement, however, was COBE's detection of slight variations at the level of one part in 100,000 and in the temperature of the CMB radiation from place to place in the sky. Observers had been diligently searching for these variations for more than two decades because they hold the key to understanding the origin of structure in the universe: how the primordial plasma evolved into galaxies, stars and planets.

Since then, scientists have employed ever more sophisticated instruments to map the temperature variations of the CMBR. The culmination of these efforts was the launch in

2001 of the Wilkinson Microwave Anisotropy Probe (WMAP), which travels around the sun in an orbit 1.5 million kilometres beyond Earth's. The results from WMAP reveal that the CMBR temperature variations follow a distinctive pattern predicted by cosmological theory: the hot and cold spots in the radiation fall into characteristic sizes. What is more, researchers have been able to use these data to precisely estimate the age, composition and geometry of the universe. The process is analogous to determining the construction of a musical instrument by carefully listening to its notes. But the cosmic symphony is produced by some very strange players and is accompanied by even stranger coincidences that cry out for explanation.

Our basic understanding of the physics behind these observations dates back to the late 1960s, when P. James E. Peebles, of Princeton University, and graduate student Jer Yu realized that the early universe would have contained sound waves. When radiation was still trapped by matter, the tightly coupled system of photons, electrons and protons behaved as a single gas, with photons scattering off electrons like ricocheting bullets. As in the air, a small disturbance in gas density would have propagated as a sound wave, a train of slight compressions and rarefactions. The compressions heated the gas and the rarefactions cooled it, so any disturbance in the early universe resulted in a shifting pattern of temperature fluctuations.

When distances in the universe grew to one thousandth of their current size—about 380,000 years after the big bang—the temperature of the gas decreased enough for the protons to capture the electrons and become atoms. This transition, called recombination, changed the situation dramatically. The photons were no longer scattered by collisions with charged particles, so for the first time they travelled largely unimpeded through space. Photons released from hotter, denser areas were more energetic than photons emitted from rarefied regions, so the pattern of hot and cold spots induced by the sound waves was frozen into the CMBR. At the same time, matter was freed of the radiation pressure that had

resisted the contraction of dense clumps. Under the attractive influence of gravity, the denser areas coalesced into stars and galaxies. In fact, the one-in-100,000 variations observed in the CMBR are of exactly the right amplitude to form the large-scale structures we see today.

Yet what was the prime mover, the source of the initial disturbances that triggered the sound waves? The question is troubling. If we imagine ourselves as an observer witnessing the big bang and the subsequent expansion, at any given point we will see only a finite region of the universe that encompasses the distance light has travelled since the 'Big Bang'.

Cosmologists call the edge of this region the 'horizon', the place beyond which we cannot see. This region continuously grows until it reaches the radius of the observable universe today. Because information cannot be conveyed faster than light, the horizon defines the sphere of influence of any physical mechanism. As we go backward in time to search for the origin of structures of a particular physical size, the horizon eventually becomes smaller than the structure.

Therefore, no physical process that obeys causality can explain the structure's origin. In cosmology, this dilemma is known as the horizon problem.

Fortunately, the theory of inflation solves the horizon problem and also provides a physical mechanism for triggering the primordial sound waves and the seeds of all structure in the universe. The theory posits a new form of energy, carried by a field dubbed the "inflaton," which caused an accelerated expansion of the universe in the very first moments after the big bang. As a result, the observable universe we see today is only a small fraction of the observable universe before inflation. Furthermore, quantum fluctuations in the inflaton field, magnified by the rapid expansion, provide initial disturbances that are approximately equal on all scales—that is, the disturbances to small regions have the same magnitude as those affecting large regions. These disturbances become fluctuations in the energy density from place to place in the primordial plasma.

Evidence supporting the theory of inflation has now been found in the detailed pattern of sound waves in the CMBR. Because inflation produced the density disturbances all at once in essentially the first moment of creation, the phases of all the sound waves were synchronized. The result was a sound spectrum with overtones much like that of a musical instrument. Consider blowing into a pipe that is open at both ends. The fundamental frequency of the sound corresponds to a wave (also called a mode of vibration) with maximum air displacement at either end and minimum displacement in the middle. The wavelength of the fundamental mode is twice the length of the pipe. But the sound also has a series of overtones corresponding to wavelengths that are integer fractions of the fundamental wavelength: one half, one third, one fourth

and so on. To put it another way, the frequencies of the overtones are two, three, four or more times as high as the fundamental frequency. Overtones are what distinguish a Stradivarius from an ordinary violin; they add richness to the sound.

The simplicity of sound waves is a hallmark of freshman physics. That same physics applied on the largest scales, is bringing us closer to unlocking the secrets of the cosmos.

In the microwave background and the distribution of galaxies, relic imprints of primordial sound waves have contributed to an extraordinarily detailed history of the universe. They provide the standard scale for resolving a great mystery.

Relativistic sound waves raced through the hot plasma that filled the universe for its first 380,000 years. That sound left an imprint that is still visible in the cosmic microwave background and in the large-scale distribution of galaxies today. Measurements of the sound waves manifested in the CMBR, coupled with a detailed understanding of the physics of sound waves in the plasma era, provide the foundation of our standard model of cosmology.

A new opportunity to track their imprint in the spatial distribution of galaxies as far back as we can observe, opens a way to solving the mystery of dark energy and its role in the history of the cosmos.

Sound waves are oscillations of compressions and rarefactions that propagate through a medium. e.g. a loudspeaker creates a local overpressure in air causing the compressed air to expand. That, in turn, compresses the neighbouring air, so that the sound wave propagates. The primordial universe was scattered with slightly over-dense, over-pressured regions that initiated the propagation of sound waves of all wavelengths. Much like the resonant sounds of a drum inform us about its shape and size, so can the details of cosmic density fluctuations tell about the universe' shape and size.

Our Big Bang universe began as hot, dense and smooth, with matter on expanding paths. By "smooth" we imply that density and velocity field deviations were negligible compared to the overall expansion of the universe. The young, seething universe was filled with a dense plasma of energetic elementary particles. Any electron trying to bind with a proton to form atoms would be instantly scattered away by photon. Atoms would not begin to form until another 380,000 years, when the universe had cooled down. (the so called "surface of last scattering"). What is left today is a much colder ensemble of nuclei, electrons, protons, neutrinos and some sort of dark matter that outweighs all the baryonic matter in the universe by a factor of 6.

When cosmologists refer to "baryonic matter" they refer to the ordinary matter made of baryons (protons and neutrons) and electrons; and when they refer to "dark matter" they mean non-baryonic matter with negligible kinetic energy. That is why it is often called cold dark matter, CDM (excluding neutrinos). Even though the constituent particles of the CDM have not yet been identified, its cosmological role is largely specified by the requirements that it be stable, immune to the strong nuclear force and electromagnetic force.

Now let us see how primordial matter was formed in the nascent universe. As mentioned earlier the young cosmos was so hot that the baryonic matter was ionized. It was dense enough so that the mean interval between consecutive scatterings of a typical photon with free electrons was much shorter than the age of the cosmos at that time. As the universe

expanded, the baryonic matter cooled and expanded, forming clusters in different sections of the universe. After 380,000 years, its temperature fell below to 3000K, allowing the nuclei and electrons to bind into stable, neutral atoms. This was the first time that simple atoms such as hydrogen were formed. The number of free electrons suddenly fell by a factor of 10^4 and the mean interval between photon-electron collisions became longer than the age of the universe. The cosmic radiation field was thus decoupled from matter, occurring in a very short period (compared to stellar formation) of only 50,000 years.

When decoupling occurred, the universe became transparent. Those photons that were colliding with electrons were now free to propagate throughout the remainder of the evolution of the universe. These photons liberated at decoupling traveling (almost) undisturbed, are what we now see as the CMBR looking back 13.8 billion years to view light that was last scattered when the universe was a thousand times smaller, a billion times denser and 1200 times hotter than it is today.

Deviations from a perfectly homogeneous universe were produced at the earliest times, possibly by quantum fluctuations during the inflationary epoch that allowed exponential expansion in the first fraction of a second. The deviations from homogeneity then grew more and more prominent throughout the rest of cosmic history, as a result of gravity imbalances they themselves produced.

The decoupled transition from ionized to neutral gas had a profound effect on the evolution of the fluctuations. Over-dense regions attracted matter more rapidly than the universal Hubble expansion could carry it away, becoming more dense with the passage of time. Similarly, baryonic matter drained away from the under-dense regions, so they became more under-dense. The over-dense regions formed primordial super clusters and nebula while the under-dense regions gave rise to the great voids of the present universe. This is shown in the contrasting sky when we look at it at night.

However, in the ionized universe before decoupling occurred, the radiation pressure imposed another key force on the baryons. The density perturbations which were spatially larger than a mean free path, the photons and plasma were coupled together to produce a uniform baryon-photon fluid.

Compression in the fluid resulted in an increase in the density and hence pressure (and temperature). The compressing plasma caused the photons to reach higher energy levels increasing radiation pressure. This opposed the compression and thus drove a consequent expansion, producing an under-dense, low pressure region that, in turn, was compressed by the surrounding fluid.

The result was a sound wave similar in all aspects to a sound wave in an ordinary fluid, except that the restoring force was the radiation pressure of the trapped photons. The radiation pressure overwhelmed gravity, hindering the fleeting gravitational instability of the post-plasma universe...

A noteworthy characteristic of the plasma sound waves in the epoch before decoupling is that their propagation speed was very high - nearly one-third the speed of light. This was because the radiation pressure and energy density of the photon field were enormous compared to that of the baryons. The photon density just prior to decoupling was that of a 3000K furnace (about 10^{12} blackbody photons per cubic centimetre). But the baryon density of the plasma was tiny - only about a thousand nucleons cm^{-3}. Sound speed scales as the square root of a restoring force per unit of inertia, and the radiation pressure of an electromagnetic field is precisely 1/3 of its energy density.

The most striking relics of the plasma epoch's sound waves are the so-called acoustic peaks in the power spectrum of the CMBR's temperature anisotropy. The temperature of the CMBR is very nearly the same (2.73K) everywhere we look. But there remain spatial variations at the level of 30μK at parts of 1 in 100000, which result largely form variations in the density of the universe at the locations where the photons last scattered before arriving at

our astronomical instruments 14 billion years later. The CMBR's temperature fluctuations recorded by the WMAP essentially shows a freeze-frame image of the sound-wave pattern at decoupling. The pattern of hot and cold spots in the map reveals an enhancement of structure on the angular scale of 0.6°.

In our quantitative analysis we shall construct the power spectrum of the temperature fluctuations by decomposing the map into spherical harmonics (using Fourier transforms) and computing the fluctuation power as a function of angular scale on the sky. The result exhibits the series of acoustic peaks first foreseen by Andrei Sakharov in 1965.

This harmonic sequence of peaks is the signature of the preferred 0.6° angular scale, just as a harmonic sequence of overtones is the signature of the fixed length of a guitar string.

How did the sound waves select a preferred angular scale?

The temperature anisotropy of the CMB is the result of a pattern of density fluctuations on a spherical surface - more accurately, a thin spherical shell of the universe - centred on us...

We are viewing that shell from a large distance. The preferred angular scale is the result of a preferred length scale on that "surface of last scattering".

That characteristic length (simply called the acoustic scale) is the distance that a sound wave propagating from a point source at the end of inflation would have travelled before decoupling-the transition that ended the plasma epoch. Since then the Hubble expansion has stretched the universe about a thousand-fold, so that now the radius of a spherical sound wave that had been propagating from the start of the plasma epoch to its end is roughly 480 million light-years. Cosmologists prefer to use a "comoving" coordinate system that dilates with the Hubble expansion. Two points otherwise at rest have a constant comoving separation, with the value given by convention as their true separation today. After decoupling, the acoustic scale is a constant comoving separation of 480Mly.

The acoustic peaks of the CMB's temperature fluctuation provide the following cosmological strong points:

- The harmonic spacing of the peaks argues strongly that the initial fluctuations in the early universe were adiabatic i.e. all the particle species varied together in density. Such joint fluctuations confirm a key prediction from inflation theory, which attributes them to primordial wrinkles in the space-time continuum.
- The relative heights of the acoustic peaks in the fluctuation power spectrum yield precision measurements of the baryon density and the density of the cold dark matter. Higher baryon density enhances the odd-numbered acoustic peaks relative to the even-numbered ones, while lower dark matter density enhances all of the peaks. The CMB data from the WMAP and from microwave telescopes on the ground have by now determined the baryon density to within 3% and the total density of baryonic plus dark matter to within 5%. Those uncertainties shrink even further when one adds astrophysical observations of the more recent universe.
- The positions of the peaks in the angular power spectrum are a manifestation of the preferred acoustic length scale. If one knows that length, one can conclude his distance from the surface of last scattering. That distance depends sensitively of the spatial curvature of the intervening universe and on the history of dark energy in the past 10 billion years. The CMB data have already confirmed that the cosmic radius of curvature, if not finite, is certainly larger than the radius of the currently visible universe.

1.2 Dark Energy and the Distance Scale

The present day acceleration of the Hubble expansion is one of the most important topics in modern cosmology. Ten years ago, studies of distant supernovae revealed this cosmic acceleration by observing that supernovae of a given redshift appeared fainter than expected. In the expanding universe the redshift z of a cosmologically distant object tells us that the cosmos has stretched by a factor of 1/1+z since the observed light began its journey. Thus the relationship of distance to redshift depends on the history of the cosmic expansion.

The unanticipated faintness of the distant supernovae can be explained if the cosmic expansion has been speeding up in recent times. One would have expected that gravity is inexorably slowing the Hubble expansion down. Instead, it looks as if the expansion is being pushed by a long-range repulsive force that has overwhelmed gravity only in the past few billion years. Einstein's cosmological constant is one possible explanation, but cosmologists attribute the phenomenon more generally to "dark energy". The small, unchanging vacuum energy density implied by Einstein's cosmological constant is just one of the several possibilities.

The claim of an accelerating cosmic expansion and the idea of a mysterious dark energy as its cause are so revolutionary that they demand particularly strong evidence. After all, distant supernovae were weak, or because something happens to their light on the way here. But additional evidence from the angular scale of the CMB acoustic peaks has convinced most cosmologists that the expansion really is accelerating. The cause however, remains unknown.

Is the dark-energy density constant in time, or is it evolving dynamically?

The key to finding out hinges on our ability to measure cosmological distances to high accuracy. Having discovered dark energy as a 10-30% effect in distance, we must now study it at a precision of better than 1%. That is an observational challenge because the measurement of distance is a long-standing problem in cosmology.

The acoustic oscillations from the early universe provide a new opportunity to measure distances at different redshifts. That is because the effect of the sound waves is not limited to the CMB photons. The sound waves also perturbed the baryons, which couple gravitationally to the dark matter. Thus the length scale that was imprinted by the sound waves persists to the present time in the clustering of matter on large scales.

It is useful to think about the physics of a single small region just after inflation, denser in plasma and dark matter than its surroundings. Because the local plasma overdensity corresponds to a region of overpressure, it launches a spherical sound wave that carries the plasma overdensity away from the centre. At the decoupling transition, the liberated photons stream away from the baryons. The sound wave stops abruptly, depositing the baryons in a spherical shell whose radius is simply the distance the sound wave has travelled. Meanwhile, the over-density in the pressureless dark matter remains at the initial location. The dark matter in the centre and the baryons in the spherical shell both seed gravitational instabilities and generate over-densities that grow more pronounced with time, eventually forming galaxies at both the centre and the shell.

Of course, the real cosmic density field is a superposition of many such shells, but the spatial correlation of galaxies is still enhanced at a comoving distance corresponding to the size of the shell at decoupling. So, galaxies in any redshift era are somewhat more likely to be separated by a comoving distance of 480 million light years than by say, 400 or 600 million light years. That preferred distance should show up as a peak – the so-called baryon acoustic oscillation peak – in the Fourier power spectrum of a sufficiently high-statistics study of positional correlations among galaxies.

Now we shall describe the origin of the baryon acoustic peak in more detail.

The radius of the 'cosmic shell' is the sound speed integrated over the time interval from inflation to decoupling. The precise calculation of the acoustic scale depends on the baryon density and on the overall density of the baryonic plus dark matter. The baryon

density affects the plasma's inertia and hence the sound speed. The total matter density affects the cosmic expansion rate and hence the duration of the plasma epoch. Fortunately, the two densities can be separately determined from the CMB power spectrum. With the WMAP data, the resulting 480 million light year comoving correlation distance is predicted to 1.3% precision. CMB measurements in the next decade should improve that precision to about 0.2%.

This method can equally be applied to standing waves instead of progressive waves. Since each Fourier mode of the perturbation evolves separately, the standing-wave representation is more suitable for precision calculation and is more easily connected to the power spectrum of the primordial fluctuations.

The length-scale of the baryon acoustic peak can be calculated from known physics and well-measured quantities and hence its apparent position in clustering surveys of galaxies at a given redshift provides a cosmic distance scale. The more distant the galaxies are from us, the smaller is the angle subtended by the preferred comoving separation of 480 million light years. By measuring the angular correlations within a large enough group of galaxies, one can measure how far away it is.

Distances in cosmology must be measured in two different ways depending on whether the separation is along the line of sight or in the transverse direction. One can infer radial separations Δr_R along the line of sight by measuring differences in cosmological redshift. One infers separations Δr_T in the transverse direction by measuring angles on the sky. Both types of measurement offer the opportunity to study the cosmological expansion history.

The acoustic scale r_A imprinted in the correlation among galaxies is, however, an intrinsically isotropic pattern. Along the line of sight, r_A produces a preferred separation Δz in redshift:

$$\Delta r_R = r_A = c\Delta z/H(z) \text{ ..... } (1.1)$$

where H(z) is the Hubble parameter at the redshift of the group of galaxies. The Hubble parameter is the cosmic expansion rate at the time corresponding to z.

In the plane normal to the line of sight, the acoustic scale produces a preferred angular separation $\Delta\theta$:

$$\Delta r_T = r_A = (1 + z)D(z)\Delta\theta, \ldots (1.2)$$

where D(z) is given by an integral involving H(z) over the period from z to the present (z = 0). D(z) is known as the angular-diameter distance.

The role of dark energy in accelerating the cosmic expansion is revealed in the evolution of H(z) and hence in the derivative of D with respect to z. By determining both H and D at different redshifts, the measurement of the baryon acoustic peak probes the history of dark energy. The method exploits the measurement of redshift and celestial angle - both of which observers can do with exquisite precision - to determine the most elusive 'cosmological distance' (to answer the long unanswered question, "How big is the universe?")

1.3 Finding the baryon acoustic peak

To measure the correlation imprinted on the galaxies by the sound waves, one needs 3D maps of their cosmic distribution. In an expanding universe, galaxy redshift surveys do that rather straightforwardly. They turn 2D images of the sky into 3D maps by making spectroscopic observations of galaxies to determine their Doppler redshifts. For galaxies distant enough that their non-Hubble motion along the line of sight can be neglected, redshift is monotonically related to distance. So a galaxy redshift survey becomes, in effect, a 3D map of the universe - although one whose radial dimension, ‘z’ has a non-trivial relation to actual distance.

Galaxy redshift surveys have been a mainstay of cosmology since the days of Edwin Hubble. They underpin most of our understanding of galaxy evolution and large-scale structure. But the detection of the baryon acoustic peak requires enormous surveys. Only the

most recent have finally mapped enough volume to see this weak large-scale feature. Not until 2005 did teams from the SDSS and the 2-Degree Field Galaxy Redshift Sky Survey announce the detection of the sought-after baryon acoustic peak.

In the correlation function of galaxies measured by the Sloan Survey, with the acoustic peak at the comoving separation predicted by WMAP measurements and the standard cosmological model, the narrowness of the acoustic peak allows its position to be determined to 4% precision. That implies a 4% measurement of the ratio between the distance to objects at z = 0.35 and our distance from the CMB's last-scattering surface at z = 1090. It also measures our absolute distance from the galaxies at z = 0.35 to about 5%.

A new generation of galaxy surveys will vastly extend our map of the cosmos. The baryon acoustic peak and its application to dark energy is currently the most prominent driver for surveys of very large cosmic volumes. The technical challenge is to acquire large numbers of faint galaxy spectra. Over the next five years, the planned new surveys will measure a million galaxies and determine the position of the baryon acoustic peak to 1% accuracy. By the end of 2030, the numbers could reach 100 million galaxies, improving the acoustic scale measurement to nearly 0.1%. That would map most of the sky out to redshifts of 2-3, where most of the dark-energy information is expected to reside.

The 'baryon acoustic peak' method has become one of the most promising ways of studying dark energy. It superbly complements the study of distant type 1a supernovae that discovered dark energy in the first place. The supernovae are easiest to measure at low redshift, where the total cosmic volume limits the acoustic peak method, which gains in precision at higher redshift. It relies on a distance scale whose well-understood physical underpinnings are validated in considerable detail by the CMB anisotropy data.

The supernovae method uses the relative observed brightness's of supernovae at different redshifts to measure a distance ratio. The baryon acoustic peak, on the other hand, calibrates the distance scale in nearly absolute terms. Using supernovae together with the

acoustic peaks in both the galaxy and CMB data will allow us to measure the cosmic distance scale to great precision across the full range of red-shifts with a solid physical calibration.

Dark energy can also be studied through its effects on the clustering of matter. Indeed it could be that the accelerating Hubble expansion, rather than being a manifestation of dark energy is actually the signal of a departure of nature from the general theory of relativity. In the correct new theory, density perturbations might behave differently from what general relativity predicts for a cosmos with the same expansion history. So a combination of precision probes that measure the growth of large structures and probes, like supernovae and acoustic peaks that measure the overall expansion rate, should let cosmologists test the physical cause of the acceleration.

This is a marvellous moment in the investigation of the cosmos. An impressively diverse set of observations has led to a standard cosmological model that is robust in its cross-checks, deeply puzzling in its ingredients, and far-reaching in its implications for fundamental physics.

Since the late 1950s, scientists have employed ever more sophisticated instruments to map the temperature variations of the CMB. The culmination of these efforts was the launch in 2001 of the Wilkinson Microwave Anisotropy Probe (WMAP), which travels around the sun in an orbit 1.5 million kilometres beyond Earth's. The results from WMAP reveal that the CMB temperature variations follow a distinctive pattern predicted by cosmological theory: the hot and cold spots in the radiation fall into characteristic sizes. What is more, researchers have been able to use these data to precisely estimate the age, composition and geometry of the universe. The process is analogous to determining the construction of a musical instrument by carefully listening to its notes. But the cosmic symphony is produced by some very strange players and is accompanied by even stranger coincidences that cry out for explanation.

2. Baryon Acoustic Oscillations

Now, we shall give substance to the explanation of the 'baryon acoustic peak', mentioned on page 20. In this derivation, the universe is slightly less than one second old. It is assumed that there exist, in thermal equilibrium, protons, neutrons, electrons, positrons and all three species of neutrino and antineutrino. We then demonstrate how, as the universe expands, the initial conditions determine the primordial abundance of the lightest nuclei.

When the universe is one second old, it's T ~ 1MeV. Photons have the blackbody distribution; there is no creation of photons once the temperature gets much below 1MeV. As a result T is proportional to 1/a. The present photon temperature is T0 = 2.73 K, which in particle physics units is 2.36×10^{-4} eV. The epoch T ~ 1MeV therefore corresponds to$1/a \sim 10^{10}$.

When specifying an epoch in the early universe the temperature is usually more convenient than the time. To specify an epoch in the fairly recent past one often gives the red-shift z of radiation emitted at that epoch. It is given by $1 + z \equiv \lambda_0/\lambda(t)=1/a(t)$ where, λ_0 is the measured wavelength and $\lambda(t)$ is the wavelength that would be measured by a co-moving observer at the time of emission.

We study the first-order perturbation of these equations. After a rather general treatment, we focus to the evolution on cosmological scales. The initial condition for such scales may be specified just after neutrino decoupling, as described earlier.

We are dealing with four fluids, but we treat the baryon–photon fluid only in the tight-coupling approximation. Using that approximation we follow the evolution of the matter density until the Newtonian description takes over. We also follow the acoustic oscillation of the baryon–photon fluid until photon decoupling. In both cases, the adiabatic initial condition is adopted.

2.1. Scalar, Vector and Tensor Modes

In Newtonian perturbation theory, we found that the Fourier components decouple. In other words, there is a separate set of equations for each **k**. We also found that there is further decoupling, so that for each **k** there is a 'scalar' mode and a 'vector' mode, with no coupling between them. As we now see, these are generic features of first-order cosmological perturbation theory, and tensor modes are also possible.

The cosmological perturbations satisfy coupled equations, containing partial derivatives with respect to time and co-moving position x^i. At first order, any one of these equations will be of the form $G = 0$, with G a linear combination of the perturbations[1]

$$G(\mathbf{x}, t) \equiv a_1(t)g_1(\mathbf{x}, t) + a_2(t)g_2(\mathbf{x}, t) + \ldots = 0. \qquad (2.1)$$

The coefficients a_n are independent of $\mathbf{x}$ because the unperturbed universe is invariant under translations. Taking the Fourier transform of both sides we have

$$G(\mathbf{k}, t) \equiv a_1(t)g_1(\mathbf{k}, t) + a_2(t)g_2(\mathbf{k}, t) + \ldots = 0, \qquad (2.2)$$

We have a separate equation for each **k**.

The following equations are of this form. They are the Newtonian continuity, Euler and Poisson equations respectively.

$$\dot{\delta}_k + \frac{k}{a}V_k = 0 \ldots \ldots \ldots \ldots \ldots \ldots \ldots ($$

$$\dot{V}_k + HV_k - \frac{k}{a}\Phi_k = \frac{k}{a}\frac{\delta P_k}{\rho}$$

$$-\frac{k^2}{a^2}\Phi_k = 4\pi G\rho\delta_k = \frac{3}{2}H^2\Omega_m(t)\delta_k$$

In the continuity and Poisson equations, G and the g_n are 3-scalars while in the Euler equation they are 3-vectors. In the relativistic case we will find that G and the g_n can also be second-rank tensors. (G and the g_n must be of the same rank, because the coefficients a_n are 3-scalars by virtue of the rotational invariance of the unperturbed universe.)

[1] In this equation, $g_n(\mathbf{x}, t)$ denotes a perturbation which may have been differentiated any number of times with respect to time and/or position coordinates. In the following equation $g_n(\mathbf{k}, t)$ denotes a perturbation which may have been differentiated any number of times with respect to t, and multiplied any number of times by components of **k**.

In the relativistic case, the equation G = 0 is obtained by perturbing an exact equation of the form '4-tensor = 0'. In practice the 4-tensor is at most of rank two, which means that G and the g_n can be 3-tensors of at most rank two. This happens for two reasons.

First, the Einstein and Maxwell field equations both involve at most second-rank 4-tensors. Second, within inflationary cosmology, all cosmological perturbations originate from the perturbations of one or more classical fields. Such fields are 4-scalars, 4-vectors or 4- tensors, and are expected to be at most rank two because tensors of higher rank are difficult to accommodate within quantum field theory, and

would correspond to fundamental particles with spin bigger than two which are not observed.

The decoupling into scalar, vector and tensor modes comes when we consider a rotation by an angle φ about the **k** direction, which changes G to some G(φ). The rotation acts on each index of G with the rotation matrix, $R_{ij} = \begin{pmatrix} cos\,\varphi & -sin\,\varphi & 0 \\ sin\,\varphi & sin\,\varphi & 0 \\ 0 & 0 & 1 \end{pmatrix}$

Suppressing those indices we can write

$$G(\phi) = \sum_m G_m e^{2\pi i m\phi} \qquad , g_1(\phi) \sum_m (g_1)_m e^{2\pi i m\phi} \qquad (2.3)$$

and so on, where m is at most equal to the rank of the 3-tensor G.

Rotational invariance requires that G(φ) = 0 independently of φ, which means that we deal with uncoupled equations:

$$G_m(\mathbf{k}, t) \equiv a_1(t)g_{1m}(\mathbf{k}, t) + a_2(t)g_{2m}(\mathbf{k}, t) + \ldots = 0. \qquad (2.4)$$

If we assume that the relevant laws of physics are invariant under parity transformation, we can choose G_m=G_{-m}, so that we need consider only m ≥ 0. The modes m = 0, 1 and 2 are called respectively the scalar, vector, and tensor modes.

The terms 'scalar', 'vector' and 'tensor' may be taken to refer to the transformation properties of G, regarded as a 2-tensor whose indices take on only two values (corresponding to components in the plane mutually perpendicular to **k**).

To make the discussion more concrete, we have to restore the indices. Consider first the scalar mode corresponding to $m = 0$. Each perturbation in this mode is invariant under rotations about $\mathbf{k}$. A 3-scalar perturbation g obviously belongs to this mode.[2]

A vector perturbation g_i belongs to the mode if it is the gradient of a scalar, so that it is of the form $g_i = gk_i$. Indeed, choosing the z-axis along $\mathbf{k}$ we find that the perturbation is then invariant under rotations about $\mathbf{k}$. Adopting the notation introduced for the Newtonian peculiar velocity, we may say that a longitudinal vector perturbation belongs to the scalar mode.

Similarly, a tensor perturbation g_{ij} belongs to the scalar mode if it is obtained from a scalar g by differentiation, corresponding to $g_{ij} = k_i k_j g$. It also belongs to the scalar mode if it is of the form $g_{ij} = g\delta_{ij}$, because the components of the tensor δ_{ij} are not affected by any rotation. Any symmetric second-rank tensor belonging to the scalar mode is a combination of these two. We met examples of both in the Newtonian case. An anti-symmetric tensor of the form $g_{ij} = \epsilon_{ijn} k_n g$ would belong to the scalar mode, but isn't encountered in practice. Higher-rank tensors of the scalar mode would have to be built from scalars using k_i, δ_{ij} and ϵ_{ijk} but are also not encountered. In summary, all scalar perturbations belong to the scalar mode, and so do those vectors and tensors that can be built from scalars using k_i, δ_{ij}, and ϵ_{ijk}.

Now we come to the vector mode. A vector g_i belongs to the vector mode if, with the z-axis along $\mathbf{k}$, it is of the form $g_i = (g_x, g_y, 0)$. In fact, a rotation (defined by R_{ij}) about the z-axis makes

$$(g_x \pm ig_y) \rightarrow e^{\pm i\varphi}(g_x \pm ig_y). \qquad (2.5)$$

Adopting the terminology used for the Newtonian peculiar velocity, we see that a vector belongs to the vector mode if it is transverse. We also note that the most general vector is the sum of a scalar and a vector mode.

2
From now on we suppress the index distinguishing the different perturbations g1 , g2 . . .. The discussion can refer to any one of them. We restore the suppressed spatial indices, so that g denotes a scalar, gi a 3-vector and gij a 3-tensor.

Tensors belonging to the vector mode have to be constructed from transverse vectors using k_i, δ_{ij} and ϵ_{ijk}. From a transverse vector g_i we get second-rank tensors in the vector mode by writing $g_{ij} = k_i g_j$ or $g_{ij} = \epsilon_{ijk} g_k$. Counting the independent components, we see that the most general anti-symmetric second-rank tensor is the sum of a scalar and a vector mode.

Finally we come to the tensor mode. A tensor g_{ij} belongs to the tensor mode if it is symmetric, traceless ($g_{ii} = 0$) and transverse ($k_i g_{ij} = 0$). This means that it is of the form,

$$g_{ij}(\boldsymbol{k}) = g_{+}(\boldsymbol{k}) e_{ij}^{+} + g_{\times}(\boldsymbol{k}) e_{ij}^{\times} \qquad (2.6)$$

where the polarization tensors $e^{+,\times}$ are defined by $e_{xx}^{+} = -e_{yy}^{+} = 1, e_{xy}^{\times} = e_{yx}^{1}$. This tensor certainly belongs to the tensor mode, because the rotation R_{ij} and $A'_{ij} = R_{in} R_{jm} A_{nm}$ imply that

$$(g_{+} \pm i g_{\times}) \rightarrow e^{\pm 2i\phi} (g_{+} \pm i g_{\times}) \qquad (2.7)$$

2.2. Perturbing the metric and energy–momentum tensors

Let us now discuss the evolution of the perturbations. **As is usual for relativistic perturbations, we will use conformal time η instead of physical time t**, and an **over-dot** will indicate d/dη instead of d/dt. To avoid confusion, one piece of guidance is convenient - equations featuring the combination (k/a) will be using physical time t, whereas those featuring k alone will be using conformal time.

2.2.1 The Metric

For the moment we leave open the gauge choice, and consider the most general first-order perturbation:

$$ds^2 = a^2(\eta)\{-(1+2A)d\eta^2 - 2B_i d\eta dx^i + [(1+2D)\delta_{ij} + 2E_{ij}]dx^i dx^j \qquad (2.8)$$

The term in square brackets specifies the spatial metric perturbation $2(D\delta_{ij} + E_{ij})$, and E_{ij} is taken to be traceless so that the separation of the two terms is unique.

The term B_i is the **shift function**; it specifies the relative velocity between the threading and the world-lines orthogonal to the slicing.

The term A is the **lapse function**, which specifies the relation between η and the proper time τ along the threading. To first order,

$$\frac{1}{a(\eta)}\frac{d\tau}{d\eta} = \sqrt{1+2A} \cong 1 + A \qquad (2.9)$$

The chosen coordinate system $x_\mu = (\eta, x_i)$ applies throughout space-time; it is a global coordinate system. In addition, at each space-time point we need a locally orthonormal coordinate system (t, r_i) (locally orthonormal frame) with the following properties: the time directions of the global and local coordinate systems are lined up to first order, and the spatial directions are lined up to zero order.

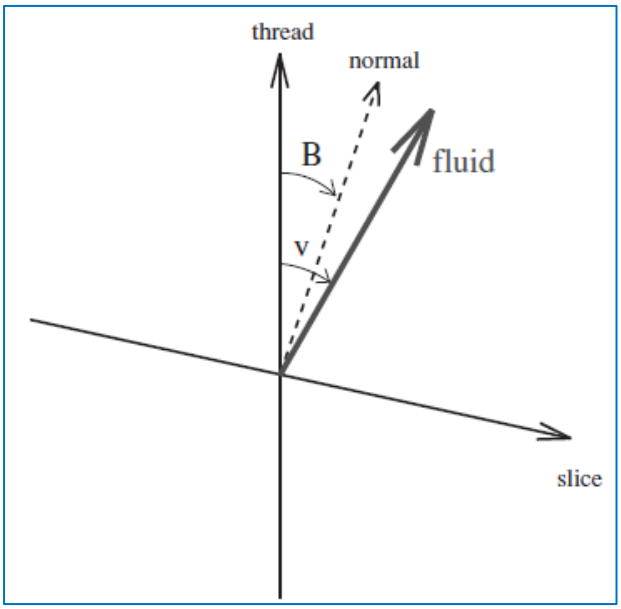

Figure 2.1
The coordinates (η, x_i) define a threading and a slicing (corresponding, respectively, to fixed x_i and fixed η). As indicated, the slicing typically isn't orthogonal to the threading. The time direction of the locally orthonormal frame considered is lined up with the time coordinate line (thread). The space directions of the locally orthonormal frame, not shown, are orthogonal to the time direction, and they coincide with the space coordinate lines to zero order in the perturbation. In the locally orthonormal frame, the velocity of a co-moving observer (fluid velocity) is **v**, and the velocity of the world-line that is normal (orthogonal) to the slices is **B**, where B_i is the shift function defined by Eq. (2.8).

From the perturbed metric (1.8), this is equivalent to,

$$dt = a(1 + A)\, d\eta \text{ (first order)}, \qquad \mathbf{(2.10)}$$

$$dr_i = a dx^i \text{ (zero order)} \qquad \mathbf{(2.11)}$$

In the locally orthonormal frame, the velocity of the worldline orthogonal to the fixed-η slice is B^i. This is illustrated above and the proof is quite simple.

Working with the coordinates (η, x^i), the 4-velocity of the worldline with velocity B_i is to first order of the form $B^\mu = B^0 (1, B^i)$. On the other hand, any 4-vector lying in the fixed-η slice is of the form $e^\mu = (0, e^i)$. One can check easily that indeed $g_{\mu\nu} B^\mu e^\nu$ vanishes to first order, for all choices of e^i.

2.2.2 The Energy-Momentum Tensor

As illustrated in Figure 8.1, the fluid velocity in the locally orthonormal frame is $v^i = dr^i/dt$. Reverting to the global coordinates, the components $u^\mu = dx^\mu/d\tau$ of the fluid 4-velocity are

$$au^0 = 1 \text{ (zero order)} \qquad (2.12)$$

$$au^i = v^i \text{ (first order)} \qquad (2.13)$$

There is no distinction between upper and lower indices for the 3-velocity v^i, but there is for the 4-velocity. Indeed, for $u_\mu = g_{\mu\nu} u^\nu$, we find

$$\frac{1}{a} u_0 = -1 \qquad zero\ order \qquad (2.14)$$

$$\frac{1}{a} u_i = v_i - B_i \qquad first\ order \qquad (2.15)$$

Using these expressions, we can work out the energy-momentum to first order:

$$T_0^0 = -(\rho + \delta\rho) \qquad 2.16$$

$$T_i^0 = (\rho + P)(v_i - B_i) \qquad 2.17$$

$$T_0^i = -(\rho + P) v^i \qquad 2.18$$

$$(P + \delta P)\delta_j^i + \Sigma_j^i \qquad 2.19$$

Raising and lowering indices has no effect on either vi or Σij because they are spatial components defined in a locally orthonormal frame. It is usual to define a dimensionless version of the anisotropic stress by Πij ≡ Σij/P.

2.2.3 The Scalar Mode

$$B_i \equiv -\frac{ik_i}{k}B, \qquad (2.20)$$

$$E_{ij} \equiv \left(-\frac{k_i k_j}{k^2}+\frac{1}{3}\delta_{ij}\right)E, \qquad (2.21)$$

$$v_i \equiv \frac{ik_i}{k}V, \qquad (2.22)$$

$$\Pi_{ij} \equiv \left(-\frac{k_i k_j}{k^2}+\frac{1}{3}\delta_{ij}\right)\Pi, \qquad (2.23)$$

In the scalar mode we can write $\delta x_i = -i(k_i/k)\delta x$.

Applying the gauge transformation

$$\widetilde{\delta B_{\mu\nu}} - \delta B_{\mu\nu} = -B_{\alpha\nu}\partial_\mu \delta x_\alpha - B_{\mu\alpha}\partial_\nu \delta x_\alpha - \delta x_\lambda \partial_\lambda B_{\mu\nu},$$

to the metric tensor gives,

$$\tilde{A} = A - (\dot{\delta\eta}) - aH\delta\eta, \qquad (2.24)$$

$$\tilde{B} = B + (\dot{\delta x}) + k\delta\eta, \qquad (2.25)$$

$$\tilde{D} = D - \frac{k}{3}\delta x - aH\delta\eta, \qquad (2.26)$$

$$\tilde{E} = E + k\delta x, \qquad (2.27)$$

Applying it to the energy–momentum tensor gives,

$$\tilde{V} = V + (\dot{\delta x}), \qquad (2.28)$$

$$\tilde{\delta} = \delta + 3(1+w)aH\delta\eta, \qquad (2.29)$$

$$\widetilde{\delta P} = \delta P - \dot{P}\,\delta\eta, \qquad (2.30)$$

$$\tilde{\Pi} = \Pi, \qquad (2.31)$$

In the second equation, we used $\dot{\rho} = -3aH(\rho + P)$along with the definitions $\delta \equiv \delta\rho/\rho$ and $w \equiv P/\rho$. We see that a slicing is needed to define the perturbations $\delta\rho$ and δP, a threading is needed to define the velocity perturbation V , and the anisotropic stress Π is gauge invariant.

2.3. Evolution of the scalar mode perturbations

The Scalar Mode

We will use the conformal Newtonian gauge which is determined uniquely by the line element,

$$ds^2 = a^2(\eta)[-(1 + 2\Psi)d\eta^2 + (1 - 2\Phi)\delta_{ij}dx^i dx^j, \qquad (2.32)$$

We will call Φ and Ψ the **gravitational potentials**. Starting with an arbitrary gauge we can indeed uniquely choose δxso that E vanishes (2.27) and then uniquely choose $d\eta$ so that B vanishes (2.25). In the conformal Newtonian gauge, slicing and threading are orthogonal, and the **worldlines** defining the latter have zero shear because the spatial part of the metric perturbation is isotropic.

The Evolution Equations

We begin with the continuity and Euler equations which follow from the Einstein field equations. Using,

$$\rho \equiv T^{00}, \ \ (for\ local\ rest\ frames), T_{ij} = P\delta_{ij} + \Sigma_{ij} \ \ and$$

$$T^{i0}\ (\rho + P)v^i, and\ also\ in\ the\ Euler\ equation\ D_\mu T^\mu_i = 0.$$

These perturbations give respectively, the two equations,

$$\dot{\delta} = -(1 + w)\left(kV - 3\dot{\Phi}\right) + 3aHw\left(\delta - \frac{\delta P}{P}\right), \qquad (2.33)$$

$$\dot{V} = -aH(1 - 3w)V - \frac{\dot{w}}{1+w}V + k\frac{\delta P}{\rho + P} - \frac{2}{3}k\frac{w}{1+w}\Pi + k\psi, \qquad (2.34)$$

where w ≡ P/ρ. The field equations give in addition

$$\delta + 3\frac{aH}{k}(1+w)V = -\frac{2}{3}\left(\frac{k}{aH}\right)^2 \Phi, \qquad (2.35)$$

$$\Pi = \left(\frac{k}{aH}\right)^2 (\Psi - \Phi), \qquad (2.36)$$

These equations involve no time derivatives and hence are constraint equations. Well after horizon entry one expects the eq. 2.35, to become simply $\delta = -\frac{2}{3}\left(\frac{k}{aH}\right)^2 \Phi$,

This expectation can be verified for the growing mode after neutrino decoupling. During matter domination Φ=Ψ, and on scales well inside the horizon, we recover Newtonian gravity with Φ and (2.37), the Poisson equation.

Initial Conditions

For each scale k, we need initial conditions to be imposed well before horizon entry. In general, that means during radiation domination. For the very long wavelength modes that enter the horizon after matter domination, we can instead take the initial epoch to be during matter domination at least for an approximate solution.

Well before horizon entry, we expect the comoving threads to have practically zero shear. Then the relation between density perturbation ρ and curvature perturbation Ψ ($\zeta = \psi - H\frac{\delta\rho}{\dot{\rho}} = \psi + \frac{1}{3}\frac{\delta\rho}{\rho+P}$) applies, with Ψ= -Φ, giving

$$\frac{\delta}{3(1+w)} = \zeta + \Phi, \qquad (2.38)$$

Also, we expect the anisotropic stress, Π to be practically zero. To be precise, we expect Π to fall off, going back in time, at least like $\left(\frac{k}{aH}\right)^2$. A single power of k would come with a spatial gradient, which isn't allowed because the three functions Π, Φ and Ψ are scalars. As a result we expect the metric perturbations Φ and Ψ to go to finite (possibly zero) values as we go back in time. Then the RHS of the equation vanishes.

Using these results or more simply by evaluating the 00-component of the Einstein equation with k=0 we arrive at the useful equation,

$$-\zeta = \Phi + \frac{2}{3}\frac{\Psi + (aH)^{-1}\dot{\Phi}}{1+w}, \qquad (2.39)$$

2.4 Separate fluids

If the cosmic fluid has a number of components, the total perturbations are,

$$\delta\rho = \sum_i \delta\rho_i, \qquad (2.40)$$

$$(\rho + P)V = \sum_i (\rho_i + P_i)V_i, \qquad (2.41)$$

$$\delta P = \sum_i \delta P_i, \qquad (2.42)$$

$$P\Pi = \sum_i P_i \Pi_i, \qquad (2.43)$$

If a component of the cosmic fluid doesn't exchange energy with its surroundings it will satisfy the continuity equation given by (2.33). And if it doesn't exchange momentum it will satisfy the Euler equation given by eq. 2.34.

We are interested in the epoch after $T{\sim}10^{-1}\,MeV$ and assume that the cosmic fluid has just the four components i= CDM (cold dark matter), B (baryons), γ(photons) and ν (neutrinos). CDM doesn't interact and has negligible pressure. It therefore satisfies the continuity and Euler equations,

$$\dot{\delta_c} = -kV_c + 3\dot{\Phi}; \qquad \dot{V_c} = -aHV_c + k\Psi \qquad (2.44)$$

Thomson scattering doesn't alter the photon energy, so that the photons and baryons satisfy the continuity equation;

$$\dot{\delta_\gamma} = -\frac{4}{3}kV_\gamma + 4\dot{\Phi}; \qquad \dot{\delta_B} = -kV_B + 3\dot{\Phi} \qquad (2.45)$$

We now adopt the 'tight-coupling approximation' for the photons and baryons. In this approximation, Thomson scattering of photons off electrons is taken to completely prevent photon diffusion. Since the electron number density everywhere, is equal to the proton number density, this gives

$$V_B = V_\gamma; \qquad \frac{\delta\left(\frac{n_B}{n_\gamma}\right)}{\frac{n_B}{n_\gamma}} = \delta_B - \frac{3}{4}\delta_\gamma = constant \qquad (2.46)$$

With the adiabatic initial condition the constant vanishes. The baryon-photon fluid is isotropic in a local rest frame and its anisotropic stress vanishes.

In the tight-coupling approximation the Euler equation for the baryon-photon fluid is

$$\dot{V}_\gamma = -aH\,(1-3\tilde{w})V_\gamma - \frac{\dot{\tilde{w}}}{1+\tilde{w}}V_\gamma + \frac{k}{3}\frac{\rho_\gamma}{\rho_B + 4/3\,\rho_\gamma}\delta_\gamma + k\Psi \qquad (2.47)$$

Here the tilde refers to the baryon-photon fluid and to a good approximation $3\tilde{w} = \rho_\gamma/(\rho_B + \rho_\gamma)$. In writing this equation we took $\delta P = \delta P_\gamma$, valid for scales above the Jeans scale.

If we ignore the neutrino perturbation (which would otherwise contribute an anisotropic stress) the tight-coupling approximation gives Ψ= Φ. Then a closed set of equations (2.46-2.47) is provided by the tight-coupling approximation together with the exact equations (2.35), (2.40)-(2.42), and (2.44). The remainder of this section focuses on this set to arrive at some rough approximations which surround the essential physics. To do this, we impose initial conditions holding well before horizon entry.

The adiabatic initial condition for the density perturbation sets ζ as constant.

It is,

$$\Phi = \Psi = -\frac{3+3w}{5+3w}\zeta \quad (before\ horizon\ entry) \quad (2.48)$$

We normally lay down the initial condition during radiation domination, so,

$$\Phi = \Psi = -\frac{2}{3}\zeta \qquad (before\ horizon\ entry) \qquad (2.49)$$

During radiation domination (2.38) gives the density contrast as,

$$\delta = \Psi = -\frac{4}{3}\zeta \qquad (before\ horizon\ entry) \qquad (2.50)$$

2.5 The matter-density transfer function

In this section we consider **the matter-dominated era**, after photon decoupling. We ignore the radiation completely so that $\Phi = \Psi$. We first show that the gravitational potential Φ_k is time independent. Then we see how to calculate a transfer function which gives its k-dependence. The calculation is vital because Φ_k has several important effects.

- It determines the course of bottom-up structure formation
- It affects the acoustic oscillation of the baryon-photon fluid
- It gives the dominant contribution to the cosmic microwave background (CMB) anisotropy on large angular scales

First we assume that no baryons are present. From Eq. 2.44 and 2.35 (or from the ij component of the Einstein equation,

$$\ddot{\Phi}_k + 6\eta^{-1}\dot{\Phi}_k = 0 \qquad (2.51)$$

This equation possesses a time-dependent solution and a decaying solution (which we ignore in this discussion).

To include the baryons we have to wait until after photon decoupling, when the baryons cease to be tightly coupled to the photons. Then, on scales in excess of the baryon Jeans scale, we have a single pressure-less fluid and arrive again at Eq. (2.51).

To calculate the time-independent Φ_k, we have to follow the evolution of the density contrast between the initial epoch and photon decoupling. If we consider those scales which are still far outside the horizon when matter domination becomes a good approximation first. Then ζ_k is constant and eq. 2.48 evaluated during matter domination gives $\Phi_k = -(3/5)\,\zeta_k$.

We therefore define a **matter transfer function by,**

$$\boldsymbol{\Phi_k = -\frac{3}{5} T(k) \zeta_k}$$

This function is time independent after photon decoupling and is close to 1 on very large scales.

For an approximate determination of T(k) it is enough only to keep the CDM, and to consider scales which are only **well inside** the horizon at decoupling. The evolution of the CDM is given in terms of the gravitational potentials by Eq. (2.44). The gravitational potentials depend on the

perturbation of all four components (namely photons, baryons, CDM and neutrinos) of the cosmic fluid. Well before horizon entry, $V_i=0$ while the δi and gravitational potentials have time-independent values given by the initial adiabatic condition. As horizon entry approaches, all of these quantities start to evolve.

Around the time of horizon entry all relevant perturbations have the same order of magnitude

$$\text{and, } \dot{\delta_c} \sim aH\delta_c \qquad (2.53)$$

The order of magnitude of the RHS is determined by the Hubble parameter which is the only scale in the problem. The precise coefficient including the sign can be calculated using either the exact equations or the tight-coupling approximation.

Well after horizon entry Eq. (2.37) applies, with $\delta\rho$ practically equal to the photon density perturbation because the neutrino perturbation has free-streamed away. The photon density contrast undergoes the decaying oscillation of the baryon-photon fluid, which means that Φ falls faster than $(aH/k)^2$ and soon becomes negligible compared with δ_c.

Combining the continuity and Euler equations for δ_c , one finds

$$\ddot{\delta}_c = aH\dot{\delta_c} = 0 \qquad (2.54)$$

With the initial conditions (2.50) and (2.53), the solution of this equation is $\delta_c \cong \zeta \ln(k/aH)$.This holds until matter-radiation equality, by which time $\delta_c \cong \zeta \ln(k\eta_{eq})$. (2.55)

At this stage δ_B/δ_C is well below its primordial value of unity, because the numerator has been undergoing a decaying oscillation while the denominator has been slowly growing. Setting $\delta_B = 0$ the density contrast is $(\rho_C/\ \rho_m)\ \delta_C$, but we can drop the pre-factor for the remainder of this discussion. Applying Eq. (2.37) and again dropping the numerical factor, we conclude that Φ_k is of order $-(k_{eq}/k)^2 \ln(k/k_{eq})\zeta_k$ when $k_{eq} = (aH)_{eq}$. This gives,

$$T(k) \cong \frac{k_{eq}^2}{k^2} ln \frac{k}{k_{eq}}, \qquad \left(k \lesssim k_{eq}\right)$$

The small non-zero value of δ_B at decoupling is an oscillating function of k, being a snapshot of the acoustic oscillation at that time. This gives a small oscillating contribution to T(k), known as **baryon acoustic oscillations (BAO),** which may ultimately prove to be a powerful standard ruler for exploring the expansion history of the universe and the properties of dark energy.

We have so far ignored the fact that neutrinos contribute a non-zero amount Ω_ν to the present matter density Ω_m. At least one neutrino species has mass m > 0.05eV. If m isn't too big the species becomes non-relativistic during matter domination. When that happens, the scale entering the horizon is 250Mpc $(1eV/m)^{1/2}$, from the conformal Friedmann equation,

$$\frac{a(\eta)}{a_{eq}} = \left(2\sqrt{2}-2\right)\left(\frac{\eta}{\eta_{eq}}\right) + \left(1-2\sqrt{2}+2\right)\left(\frac{\eta}{\eta_{eq}}\right)^2 \qquad and \qquad z_{nr} = \frac{m_a}{5\times10^{-4}eV} \lesssim 2000.$$

On much smaller scales the density of species free-streams away, reducing the matter-density contrasts by a fractional amount of order Ω_ν/Ω_m where Ω_ν is the contribution of just this species. On much larger scales there is no significant reduction. For this effect to be observable the mass has to be much has to be much bigger than 0.05eV, requiring the mass of two or all three species to be practically the same.

The present observable constraint, $\Sigma m_i < 1eV$, is obtained by fitting both galaxy distribution data, which is sensitive to the above reduction, and CMB anisotropy data. With future improvements in both these types of data, it will probably be possible to infer at least the heaviest neutrino mass.

To obtain an accurate transfer function over the full range of scales, more numerical derivations are required which are beyond the scope of this discussion. If we assume that neutrinos have zero mass, the result shown in the figure is obtained using "CMB-fast" code program. The baryon oscillations can just be identified, and the approach to the asymptotic region k>>aH is clearly observed.

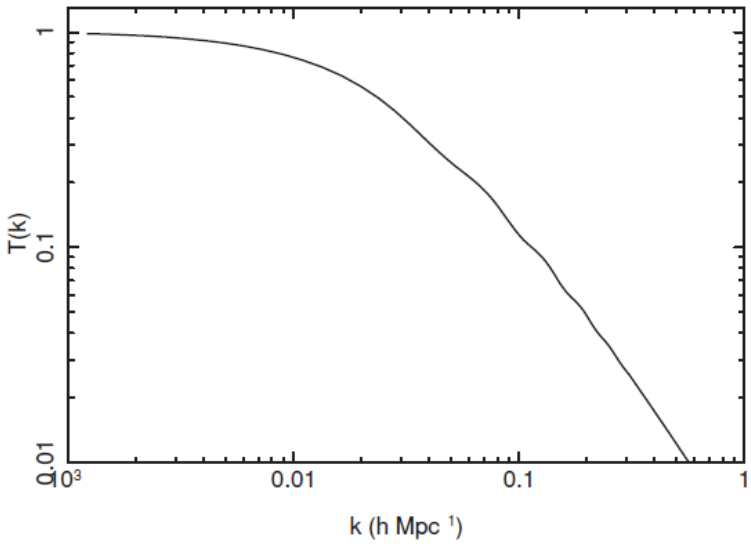

Figure 2.2 The Adiabatic Transfer Function for Standard Cosmology

2.6. Acoustic Oscillations

Until photon decoupling, the baryons and photons for a tightly-coupled fluid, supporting a standing-wave acoustic oscillation. The photons then travel freely, but imprinted on there is a snapshot of the oscillation as it existed just before decoupling. This gives rise to the **peak structure** in the CMB anisotropy. The same peak structure gives the small oscillation in the matter transfer function.

Now, we form our key discussion in the light of the tight-coupling approximation. To make the formulae useful for the CMB discussion, we shall sometimes translate the co-moving wave number k into the multi-pole $\ell = \mathcal{k}\eta_0$ of the CMB anisotropy.

Combining the continuity and Euler equations gives an equation governing the acoustic oscillation of the baryon-photon fluid. It is,

$$\frac{1}{4}\ddot{\delta}_{\gamma k} + \frac{1}{4}\frac{\dot{R}}{1+R}\dot{\delta}_{\gamma k} + \frac{1}{4}k^2c^2\delta = F_k(\eta) \qquad (2.57)$$

In this equation,

$$F_k(\eta) \equiv -\frac{k^2}{3}\Psi_k(\eta) + \frac{\dot{R}(\eta)}{1+R(\eta)}\dot{\Phi}_k(\eta) + \ddot{\Phi}_k(\eta) \quad (2.58)$$

$$c_s^2(\eta) \equiv \frac{\dot{P}}{\dot{\rho}} \cong \frac{\dot{P}_\gamma}{\rho_\gamma + \dot{P}_B} = \frac{1}{3[1+R(\eta)]} \quad (2.59)$$

$$R(\eta) \equiv \frac{3\rho_B}{4\rho_\gamma} \quad (2.60)$$

In the regime where c_s is slowly varying, Eq. (2.57) is the equation of a forced oscillator, with a driving term F and speed of sound c_s. We will ignore the small damping of this oscillation provided by the 2nd term of Eq. 2.57 because it is negligible.

The two constraint equations determine F in terms of the perturbations of the neutrinos, the CDM and the baryon-photon fluid itself.

As the 1st two terms vary slowly, the angular frequency of the driving term is kc_s. This is also the frequency of the oscillation, which has the form factor

$$\frac{1}{4}\delta_{\gamma\boldsymbol{k}}(\eta) = A_k(\eta) + B_k(\eta)\,cos[kr_s(\eta)] + C_k(\eta)\,sin[kr_s(\eta)] \qquad (2.61)$$

With slowly varying coefficients A_k , B_k and C_k.

The coefficient A_k corresponds to the oscillation being off-centre, owing to the effect of the non-oscillating contributions to the driving term. After matter domination, it corresponds to the non-oscillating solution of Eq. 2.57,

$$A_k(\eta) = -[1 + R(\eta)]\Phi_k \qquad (2.62)$$

The slowly varying quantity r_s is the distance that sound has had time to travel since a much earlier time, idealized as η=0. It is called the sound horizon and is given by

$$\boldsymbol{r_s(\eta) = \int_0^{\eta} c_s(\eta) d\eta} \qquad \boldsymbol{(2.63)}$$

At early times R≈0, $c_s=1/\sqrt{3}$ and $r_s=c_s\eta$. The baryon fraction increases with time,

$$R(\eta) = \frac{3}{4} f_B (1 - R_\nu)^{-1} \frac{z_{eq}}{z(\eta)} \qquad (2.64)$$

Where $f_B \equiv \frac{\rho_B}{\rho_m}$ and $R_\nu \equiv \frac{\rho_\nu}{\rho_r} = 0.40$. The sound horizon also increases with time. Using,

$$\frac{a(\eta)}{a_{eq}} = \left(2\sqrt{2} - 2\right)\left(\frac{\eta}{\eta_{eq}}\right) + \left(1 - 2\sqrt{2} + 2\right)\left(\frac{\eta}{\eta_{eq}}\right)^2$$, Eqs. (2.59)and(2.63),

$$r_s(\eta) = \frac{2}{3k_{eq}}\sqrt{\frac{6}{R_{eq}}} \ln\left(\frac{\sqrt{1 + R(\eta)} + \sqrt{R(\eta) + R_{eq}}}{1 + \sqrt{R_{eq}}}\right) \qquad (2.65)$$

At decoupling, R and r_s are given by,

$$R = \frac{3}{4} f_B \left(1 - f_\nu\right)^{-1} \frac{z_{eq}}{z_{ls}} = 29\Omega_B h^2 \cong 0.65 \qquad r_s = 1.5 \times 10^2 \text{ Mpc} \qquad (2.66)$$

We need to check if c_s is indeed slowly varying on the timescale of the oscillations, corresponding to $(c_s)'/c_s \ll k c_s$. If this requirement is satisfied at decoupling it is satisfied at earlier times as well. Remembering that R_{ls}~1 it corresponds to $k\eta_{ls} \gg 1$ or $\ell \gg 70$.

2.7. Diffusion damping

In modern cosmological theory, diffusion damping, also called photon diffusion damping, is a physical process which reduced density inequalities (anisotropies) in the early universe, making the universe itself and the cosmic microwave background radiation (CMBR) more uniform. Around 300,000 years after the 'Big Bang', during the time of recombination, diffusing photons travelled from hot regions of space to colder regions, equalising temperatures. This effect, along with baryon oscillations, the Doppler effect and gravitation, was responsible for the eventual formation of galaxies and galaxy clusters – the dominant large scale structures observed in the universe. Diffusion damping is a damping by diffusion, and not *of* diffusion. The strength of diffusion damping is chiefly governed by the distance (the diffusion length) that photons travel before being scattered.

Between the epoch of decoupling and the epoch of reionisation, the universe is almost transparent to photons. As we shall discuss further, the probability that a given photon scatters after reionisation is expected to be significantly less than 1, and so, to a useful approximation, we can say that all CMB photons that we see, originate on the surface of a precisely defined sphere around us – the surface of last scattering. The cosmic microwave background anisotropy comes partly from the anisotropy already present at last scattering, and partly from the additional anisotropy caused by gravity since then. With critical mass density, it is realised that the latter effect depends only on conditions at last scattering. As a result, each angular scale explores the linear scale that it subtends at the surface of last scattering, to the extent that reionisation may be ignored.

This surface lies practically at the particle horizon, whose comoving distance is $2H_0^{-1}\,\theta$, or

$$\frac{x}{100h^{-1}Mpc} \simeq \frac{\theta}{1^0} \qquad (2.67)$$

This is the relationship between linear and angular scale, ignoring reionisation and the finite thickness of the last-scattering surface. A multipole order of ℓ corresponds to an angular scale of order $\theta \simeq \frac{1}{\ell}$ and so the ℓth multipole probes the comoving scale x and the comoving wavenumber k, given by

$$k^{-1} \simeq x \simeq \frac{2}{H_0\ell} = 6000h^{-1}\ell^{-1}Mpc. \qquad (2.68)$$

In reality, the last-scattering surface has a finite thickness, which comes from the fact that, at any epoch, a photon has had time to diffuse a certain distance. This distance is called the *Silk scale*, and its value at decoupling is the thickness of the surface of last scattering. We shall now estimate the Silk scale.

Before decoupling, the photons move about randomly, as they exhibit Thomson scattering with electrons. The mean time between collisions is $t_c \sim (n_e \sigma_T)^{-1}$, where n_e is the electron number density and σ_T is the Thomson-scattering cross-section. The average number of steps in time t is $N = t/t_c$, and in that time a photon diffuses a distance $d \sim \sqrt{N} t_c \sim (t t_c)^{\frac{1}{2}}$.

At decoupling, with $t \sim 1/H$, this is the thickness of the surface of last scattering. A careful estimate using the transport equations gives a thickness of order

$$7\Omega_0^{-\left(\frac{1}{2}\right)} h^{-1} Mpc$$

Corresponding to $\ell \sim 10^3$. As a result, the anisotropy will be wiped out on much smaller scales, for much larger ℓ.

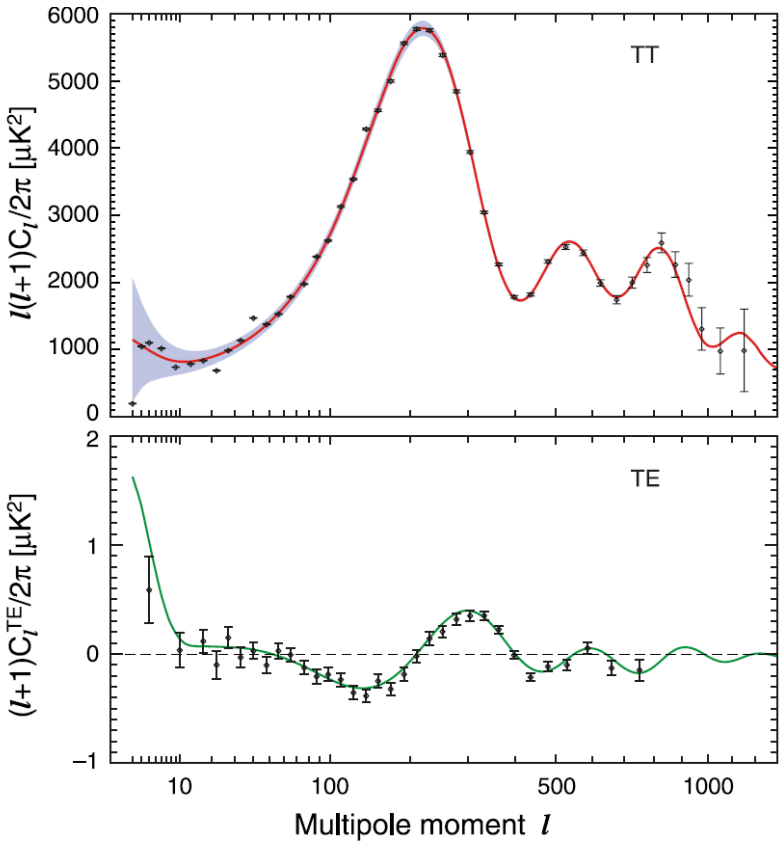

3. Discussion

The fact that the universe is expanding - about every point in space - can be a difficult concept to grasp. The analogy of an expanding balloon may be helpful: Imagine residing in a curved flatland on the surface of a balloon. As the balloon is blown up, the distance between all neighbouring points grows; the two-dimensional universe grows but there is no preferred centre.

100,000 years after the Big Bang, the temperature of the universe had dropped sufficiently for electrons and protons to combine into hydrogen atoms, p + e --> H. From this time onwards, radiation was effectively unable to interact with the background gas; it has propagated freely ever since, while constantly losing energy because its wavelength is stretched by the expansion of the universe. Originally, the radiation temperature was about 3000 degrees Kelvin, whereas today it has fallen to only 3K.

Observers detecting this radiation today are able to see the universe at a very early stage on what is known as the `surface of last scattering'. Photons belonging to the cosmic microwave background have been travelling towards us for over ten billion years, and have covered a distance of about 10^{24} miles.

If fluctuations in the distribution of matter in the primordial universe have equal power on all spatial scales, cosmologists say that their power spectrum is 'scale-invariant'. This is characterised with a parameter known as the spectral index, ns. For a perfectly scale-invariant spectrum, ns = 1. If ns is smaller than 1, it means that fluctuations on larger scales are dominant, since they are more abundant (in terms of their cumulative power) than those on smaller scales; vice versa, if ns is larger than 1, fluctuations on small scales are the dominant ones.

3.1 Nucleosynthesis and the shortcomings of standard cosmology

Prior to about one second after the Big Bang, matter - in the form of free neutrons and protons - was very hot and dense. As the universe expanded, the temperature fell and some of these nucleons were synthesized into the light elements: deuterium (D), helium-3, and helium-4. Theoretical calculations for these nuclear processes predict, for example, that about a quarter of the universe consists of helium-4, a result which is in good agreement with current stellar observations.

The heavier elements, of which we are partly made, were created later in the interiors of stars and spread widely in supernova explosions.

The standard Hot Big Bang model also provides a framework in which to understand the collapse of matter to form galaxies and other large-scale structures observed in the universe today. At about 10,000 years after the Big Bang, the temperature had fallen to such an extent that the energy density of the universe began to be dominated by massive particles, rather than the light and other radiation which had predominated earlier. This change in the form of the main matter density meant that the gravitational forces between the massive particles could begin to take effects, so that any small perturbations in their density would grow. Ten billion years later we see the results of this collapse.

The standard cosmology, then, provides a framework for understanding galaxy formation, but it does not tell us about the origin of the primordial fluctuations required at 10,000 years. We must seek answers to questions like these from earlier epochs in the history of the universe.

Despite the self-consistency and remarkable success of the standard Hot Big Bang model in our discussion of the evolution of the universe back to only one hundredth of a second, a number of unanswered questions remain regarding the initial state of the universe.

The flatness problem

Why is the matter density of the universe so close to the unstable critical value between perpetual expansion and re-collapse into a Big Crunch?

The horizon problem

Why does the universe look the same in all directions when it arises out of causally disconnected regions? This problem is most acute for the very smooth cosmic microwave background radiation.

The density fluctuation problem

The perturbations which gravitationally collapsed to form galaxies must have been primordial in origin; from whence did they arise?

The dark matter problem

Of what stuff is the universe predominantly made? Nucleosynthesis calculations suggest that the dark matter of the universe does not consist of ordinary matter - neutrons and protons?

The cosmological constant problem

Why is the cosmological constant, 120 orders of magnitude smaller than naively expected from quantum gravity?

The singularity problem

The cosmological singularity at t=0 is an infinite energy density state, so general relativity predicts its own breakdown.

There are strong reasons to believe that the fluctuations which seeded the large-scale structures of the universe must have been primordial in origin, that is, associated with some of the very earliest times after the Big Bang. The primary candidates at the present time are (1) topological defects, such as cosmic strings and textures, or (2) inflationary scenarios.

It possible, thus, to carry on in the field of this study in order that we may quantify measurable outcomes to the shortcomings listed. This can be only furthered by the rigorous and dedicated recording of data from CMBR probes, which are mentioned .

3.2 WMAP data and results

The Wilkinson Microwave Anisotropy Probe (WMAP) observatory has successfully completed seven years of observations with no significant performance degradation. A full set of sky maps for the seven year (2001-2008) data span have been generated and are available for analysis.

These maps were generated with an updated masking procedure that simplifies the map-making procedure and allows the creation of a single full-sky noise correlation matrix describing the noise correlation over the entire sky for the reduced noise resolution sky maps. The WMAP results significantly reduce the uncertainties for numerous cosmological parameters relative to earlier results.

The following figures display the seven-year band average Stokes I maps and the differences between these maps and maps earlier published. The difference maps have been adjusted to compensate for the slightly different gain calibrations and dipole signals used in the different analysis. The small galactic plane features in the K, Ka and Q band difference maps arise from the slightly different calibrations and small changes in the effective beam shapes. The dipole measured from the seven year data show no significant changes from that of earlier results.

The left column displays the seven-year average maps of the CMBR sky, all of which have a common dipole signal removed. The right column displays the difference between the seven-year average maps and the previously published five-year average maps, adjusted to take into account the slightly different dipoles subtracted in the seven-year and five-year analyses and the slightly differing calibrations. All maps have been smoothed with a 1° FWHM Gaussian kernel. The small galactic plane signal in the difference maps arises from difference in calibration and beam symmetrisation between the two periods of processing.

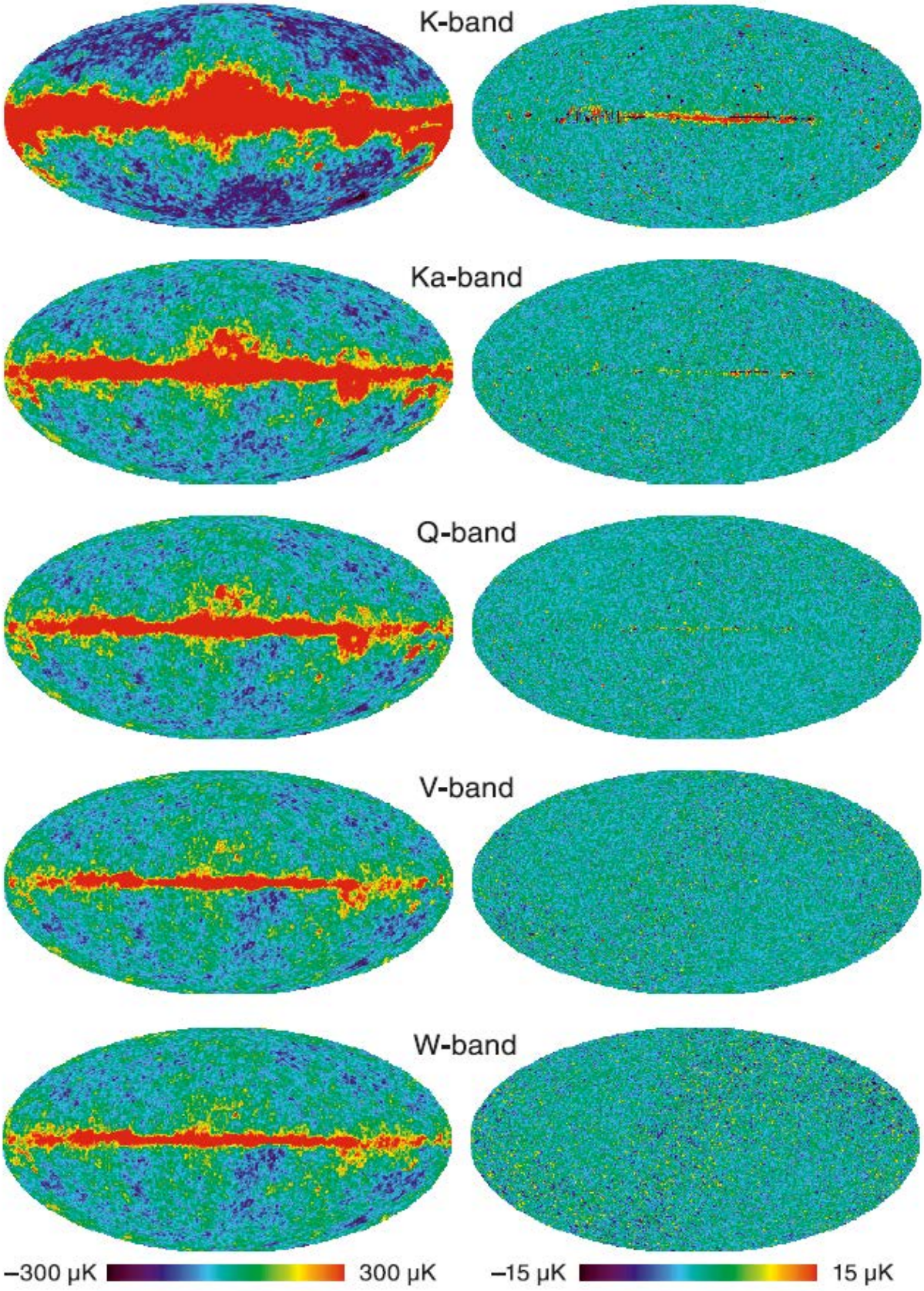

Figure 3.1 – Plots of the Stokes I maps in Galactic coordinates. The left column displays the seven-year average maps, all of which have a common dipole signal removed. The right column displays the difference between the seven-year average maps and previously published maps, adjusted to take into account the slightly different dipoles subtracted in the seven-year and five-year analyses and the slightly differing calibrations. The small Galactic plane signal in the difference maps arises from the difference in calibration (0.1%) and beam symmetrization between the five-year and seven-year processing.

4. Conclusion

The Cosmic Background Explorer satellite was launched twenty five years after the discovery of the microwave background radiation in 1964. In spectacular fashion in 1992, the COBE team announces that they had discovered `ripples at the edge of the universe', that is, the first sign of primordial fluctuations at 100,000 years after the Big Bang. These are the imprint of the seeds of galaxy formation.

These appear as temperature variations on the full sky picture that COBE obtained. They are at the level of only one part in one hundred thousand. Viewed in reverse the universe is highly uniform in every direction lending strong support for the cosmological principle.

Further, the data obtained from the Wilkinson Microwave Anisotropy Probe (WMAP) have allowed us to achieve great precision while quantifying the predicted spectrum for the best fit minimal six-parameter ΛCDM model as stated in section 2.7.

Thus, I believe that data from the WMAP have allowed us to propose a proper model for the creation of the universe. It is possible for us to examine the results in detail in this respect, and further our study. However, as I was faced with technical limitations, namely a lack of laboratory equipment to observe the CMB sky, I was incapable of quantifying any results of my own. I propose that it would be of great significance if we could set up an observatory in this regard in future in order to gather our own data and not having to rely on sources, as was done here.

For the time being, the seven-year WMAP data remains to be a sound inference for our study and has been used in the latter content of this thesis. So, we can further our work as necessary while using this data and make any changes with later and more accurate observations of the sky.

4.1 Ripples at the edge of the universe

This thumbprint image shows the temperature of the universe in all directions projected onto a plane (similar to a map of the earth):

1. The raw temperature map (top) has a large diagonal asymmetry due to our motion with respect to the cosmic microwave background - a Doppler shift.

2. The temperature fluctuations after subtraction of the velocity contribution, showing primordial fluctuations and a large radio signal from nearby sources in our own galaxy (the horizontal strip).

3. The primordial fluctuations after subtraction of the galaxy signal.

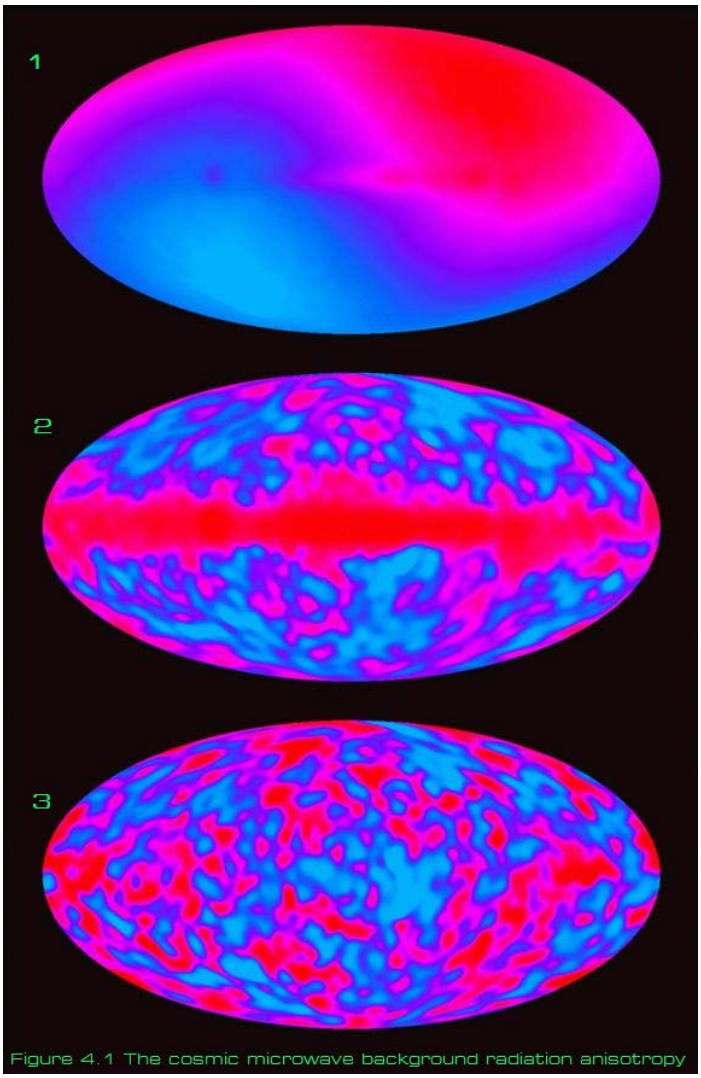

Figure 4.1 The cosmic microwave background radiation anisotropy

4.2 Prospective study using WMAP research data

When cosmologists study the formation and evolution of cosmic structure in the universe, they plot the relative number of cosmic structures on different sizes in a power spectrum. The shape of this graph reveals the 'power' of structures that populate the universe on each scale. For example, there may be very few structures at very large scales. But counting all of these very large structures' contributions together gives a measure of their cumulative power. If the power is to be matched with only smaller structures, a much larger number of them are needed.

Cosmic structures – stars, galaxies, galaxy clusters – grow under the influence of gravity, which causes them to become denser and denser. However, other forces may act against the attractive pull of gravity; for example, the expansion of the universe or radiation pressure – the pressure force exerted by photons. Every structure that we observe in the universe is the result of the balance between all these effects during the infancy of the universe.

The WMAP data remains one of the cornerstone data sets used for testing the cosmological models and the precision measurement of their parameters. Figure 4.2 displays the binned TT and TE angular power spectra measured from the seven-year WMAP data (Larson et al. 2010), along with the predicted spectrum for the best fit minimal six-parameter flat _CDM model. The overall agreement is excellent, supporting the validity of this model. Figure 4.2 tabulates the parameter values for this model using WMAP data alone, and in combination with other data sets. Details of the methodology used to determine these values are described in Larson et al. (2010) and Komatsu et al. (2010).

The seven-year WMAP results significantly reduce the uncertainties for numerous cosmological parameters relative to the five-year results. The uncertainties in the densities of baryonic and dark matter are reduced by 10% and 13% respectively. When tensor modes are included, the upper bound to their amplitude, determined using WMAP data alone is nearly

20% lower. By combining WMAP data with the latest distance measurements from Baryon Acoustic Oscillations (BAO) in the distribution of galaxies (Percival et al. 2009) and Hubble constant measurements (Riess et al. 2009), the spectral index of the power spectrum of primordial curvature perturbations is $\eta_s = 0.963 \pm 0.012$, excluding the Harrison-Zel'dovich-Peebles spectrum by more than 3σ.

The reduced noise obtained by using the seven-year data set yields a better measurement of the third acoustic peak in the temperature power spectrum. This measurement, when combined with external data sets, leads to better determinations of the total mass of neutrinos, Σm_ν , and the effective number of neutrino species, N_{eff}, as presented in Table 4.2.

Table 4.2

Description	Symbol	*WMAP* -only	*WMAP* +BAO+H_0
Parameters for Standard ΛCDM Model [a]			
Age of universe	t_0	13.75 ± 0.13 Gyr	13.75 ± 0.11 Gyr
Hubble constant	H_0	71.0 ± 2.5 km/s/Mpc	$70.4^{+1.3}_{-1.4}$ km/s/Mpc
Baryon density	Ω_b	0.0449 ± 0.0028	0.0456 ± 0.0016
Physical baryon density	$\Omega_b h^2$	$0.02258^{+0.00057}_{-0.00056}$	0.02260 ± 0.00053
Dark matter density	Ω_c	0.222 ± 0.026	0.227 ± 0.014
Physical dark matter density	$\Omega_c h^2$	0.1109 ± 0.0056	0.1123 ± 0.0035
Dark energy density	Ω_Λ	0.734 ± 0.029	$0.728^{+0.015}_{-0.016}$
Curvature fluctuation amplitude, $k_0 = 0.002$ Mpc^{-1} [b]	$\Delta^2_{\mathcal{R}}$	$(2.43 \pm 0.11) \times 10^{-9}$	$(2.441^{+0.088}_{-0.092}) \times 10^{-9}$
Fluctuation amplitude at $8h^{-1}$ Mpc	σ_8	0.801 ± 0.030	0.809 ± 0.024
Scalar spectral index	n_s	0.963 ± 0.014	0.963 ± 0.012
Redshift of matter-radiation equality	$z_{\rm eq}$	3196^{+134}_{-133}	3232 ± 87
Angular diameter distance to matter-radiation eq.[c]	$d_A(z_{\rm eq})$	14281^{+158}_{-161} Mpc	14238^{+128}_{-129} Mpc
Redshift of decoupling	z_*	$1090.79^{+0.94}_{-0.92}$	$1090.89^{+0.68}_{-0.69}$
Age at decoupling	t_*	379164^{+5187}_{-5243} yr	377730^{+3205}_{-3200} yr
Angular diameter distance to decoupling [c,d]	$d_A(z_*)$	14116^{+160}_{-163} Mpc	14073^{+129}_{-130} Mpc
Sound horizon at decoupling [d]	$r_s(z_*)$	$146.6^{+1.5}_{-1.6}$ Mpc	146.2 ± 1.1 Mpc
Acoustic scale at decoupling [d]	$l_A(z_*)$	302.44 ± 0.80	302.40 ± 0.73
Reionization optical depth	τ	0.088 ± 0.015	0.087 ± 0.014
Redshift of reionization	$z_{\rm reion}$	10.5 ± 1.2	10.4 ± 1.2
Parameters for Extended Models [e]			
Total density [f]	$\Omega_{\rm tot}$	$1.080^{+0.093}_{-0.071}$	$1.0023^{+0.0056}_{-0.0054}$
Equation of state [g]	w	$-1.12^{+0.42}_{-0.43}$	-0.980 ± 0.053
Tensor to scalar ratio, $k_0 = 0.002$ Mpc^{-1} [b,h]	r	< 0.36 (95% CL)	< 0.24 (95% CL)
Running of spectral index, $k_0 = 0.002$ Mpc^{-1} [b,i]	$dn_s/d\ln k$	-0.034 ± 0.026	-0.022 ± 0.020
Neutrino density [j]	$\Omega_\nu h^2$	< 0.014 (95% CL)	< 0.0062 (95% CL)
Neutrino mass [j]	$\sum m_\nu$	< 1.3 eV (95% CL)	< 0.58 eV (95% CL)
Number of light neutrino families [k]	$N_{\rm eff}$	> 2.7 (95% CL)	$4.34^{+0.86}_{-0.88}$

[a]The parameters reported in the first section assume the 6 parameter flat ΛCDM model, first using *WMAP* data only (Larson et al. 2010), then using *WMAP* +BAO+H_0 data (Komatsu et al. 2010). The H_0 data consists of a Gaussian prior on the present-day value of the Hubble constant, $H_0 = 74.2 \pm 3.6$ km s^{-1} Mpc^{-1}(Riess et al. 2009), while the BAO priors on the distance ratio $r_s(z_d)/D_{\rm V}(z)$ at $z = 0.2,\ 0.3$ are obtained from the Sloan Digital Sky Survey Data Release 7 (Percival et al. 2009). Uncertainties are 68% CL unless otherwise noted.

[b]$k = 0.002$ Mpc^{-1} $\longleftrightarrow$ $l_{\rm eff} \approx 30$.

References:

1. Bucaille, M. (1978). *The Bible, The Quran and Science*. North American Trust
2. Liddle, A., *An Introduction to Modern Cosmology*, Second Edition (2003)
   Hu, W., Sugiyama, N., *Small Scale Cosmological Perturbations* (1996)
3. Lyth, David H., and Andrew R. Liddle. *The Primordial Density Perturbation : Cosmology, Inflation and the Origin of Structure*. Leiden: Cambridge University Press, 2009
4. Hlozek, R., Cortˆes, M. Clarkson, C., Bassett, B. *General Relativity and Gravitation*, 40: 285-300
5. White, M. *Astroparticle Physics* (2005)
6. Bassett, B. A., Fantaye, Y. T., Hlozek, R. A., and Kotze, J. ArXiv: 0906.0993
7. http://www.qsl.net/n9zia/wireless/appendixF.html
8. http://www.astro.ucla.edu/~wright/cosmo_02.htm
9. http://physics.aps.org/articles/v4/9
10. http://arxiv.org/abs/astro-ph/9508159
11. http://arxiv.org/abs/1001.4538
12. http://www.cfa.harvard.edu/~aas/tenmeter/cmb.htm
13. http://adsabs.harvard.edu/abs/1993ApJ...419....1K
14. ned.ipac.caltech.edu/level5/Glossary/Essay_lss.html
15. www.astro.ubc.ca/people/scott/cmb.html
16. lambda.gsfc.nasa.gov/product/cobe/firas_image.cfm
17. cmb.as.arizona.edu/~eisenste/acousticpeak/acoustic_physics.html
18. ned.ipac.caltech.edu/level5/Kosowsky2/Kosowsky5.html
19. chrisnorth.github.io/planckapps/Simulatoresearch/gr/public/index.html, 1996 Cambridge University